

Supplemental Methods

Table S1: Covariate sources and definitions.

Table S2: Disease phenotype codes and definitions.

Table S3: Genetic variants associated with TKV beyond genome-wide significance.

Table S4: Summary of genome-wide association studies used in two-sample Mendelian randomization analyses.

Table S5: Baseline demographic characteristics

Table S6: Discrimination, calibration, and likelihood ratio test assessing CKD stage G3+ risk prediction performance of eGFR and uACR compared to model incorporating TKV measurements.

Table S7: Improvement in category-free risk reclassification when TKV, htTKV, or BSA-TKV were added to a baseline model of eGFR and uACR.

Table S8: Inverse variance weighted, weighted median, and MR Egger regression results for each outcome association using all variants.

Table S9: Instrument strength, intercept test, and heterogeneity test results for each TKV-outcome association.

Table S10: Inverse variance weighted, weighted median, and MR Egger results for each TKV-outcome association, excluding outlier variants identified by MR-PRESSO and BMI or BSA-associated SNPs.

Table S11: Nonlinear MR tests of nonlinearity and heterogeneity.

Table S12: Inverse variance weighted, weighted median, and MR Egger results for each genetically predicted exposure and TKV association.

Table S13: Instrument strength, intercept test, and heterogeneity test results for each exposure-outcome association.

Table S14: Inverse variance weighted, weighted median, and MR Egger results for each genetically predicted exposure and TKV association, excluding outlier variants identified by MR-PRESSO.

Figure S1: Histogram of TKV, htTKV, or BSA-TKV.

Figure S2: Association of TKV with all cases of kidney and cardiovascular disease outcomes.

Figure S3: Association of htTKV with kidney and cardiovascular disease outcomes and measures.

Figure S4: Association of BSA-TKV with kidney and cardiovascular disease outcomes and measures.

Figure S5: Nonlinear association of TKV with eGFR_{Cr} and incident cases of CKD stage G3+.

Figure S6: Nonlinear association of htTKV with kidney and cardiovascular disease outcomes and measures

Figure S7: Nonlinear association of BSA-TKV with kidney and cardiovascular disease outcomes and measures.

Figure S8: Calibration plot comparing observed and predicted risk when BSA-TKV is incorporated in a baseline model with eGFR and uACR.

Figure S9: Association of BSA-TKV thresholds with incident CKD stage G3+ split by age, sex, and BMI subgroups.

Figure S10: Histogram and summary statistics of BSA-TKV thresholds identified from 1,000 iterations of bootstrap resampling in three different univariable and multivariable settings.

Supplemental Methods

eGFR and uACR Assessment in UK Biobank

Race-free eGFR (mL/min/m²) was calculated using serum creatinine (mg/dL) and cystatin C (mg/L) according to the 2021 CKD-EPI creatinine (eGFR_{Cr}) and creatinine-cystatin C (eGFR_{CrCys}) equations. uACR (mg/mmol) was calculated by dividing urine microalbumin (mg/L) and urine creatinine (mmol/L). Biochemistry and urine data were winsorized according to reportability limits. Individuals with undetectable urine albumin were assigned the lower limit of detection (6.7 mg/L).

Covariates

Participants' age, alcohol consumption, and smoking status were collected from self-report questionnaire. Image processing protocol version and assessment centre were included as nuisance factors. Genetic sex and genetic principal components (PC) were obtained from genotype data. Height (m), weight (kg), and BMI (kg/m²) were collected from physical measurements. Missing height and weight were assigned values from overlapping data fields in UK Biobank (Table S1).

Systolic blood pressure (SBP), hypertension, HbA1c and diabetes mellitus (DM) were also included as additional covariates. SBP (mmHg) measurements were amalgamated from both manual and automated readings. HbA1c (mmol/mol) was collected from blood biochemistry data and winsorized according to reportability limits. HbA1c mmol/mol was converted to % using the conversion factor (1/10.929) + 2.15. Hypertension was defined by ICD10 phocode 401 (Table S2). DM was defined by ICD10 phocode 250.

Disease Outcome Assessment

Disease outcomes were assessed according to eTable 2. Incident cases and time-to-event were defined based on time of imaging. Analyses of incident chronic kidney disease (CKD) stage G3+ and acute kidney injury (AKI) excluded individuals with any baseline eGFR < 60 mL/min/m², uACR > 30 mg/mmol, or records of CKD stage G3+ and AKI prior to time of imaging. Analyses of incident cardiovascular outcomes excluded individuals who meet any of the listed definitions for ischemic heart or cerebrovascular diseases prior to time of imaging. Control groups for CKD stage G3+ and AKI excluded individuals with any codes for CKD (ICD10 N18.0 to N18.5), AKI (ICD10 N17.0 to N17.9), dialysis (ICD10 Y60.2, Y84.1, Z49.0, Z49.1, Z49.2, Z99.2; OPCS4 X40 to X42), algorithmically defined end-stage kidney disease (UKB FID 42027), eGFR <60 mL/min/m², or uACR >= 3 mg/mmol. Control groups for cardiovascular outcomes excluded individuals who meet any of the listed definitions for ischemic heart and cerebrovascular disease.

Nonlinear Association Analyses

TKV measurements underwent nonlinearity testing and appropriate transformation using the multivariate fractional polynomial method (R mfp package v 1.5.2.2).¹ Continuous covariates also underwent nonlinearity testing and transformation to optimize model adjustment accuracy. This method involves an iterative selection of the best-fitting model across a series of fractional polynomial transformations, comparing to the linear model or the previous model of best fit as the null hypothesis. The optimal transformation was selected based on 1) significance of nonlinearity followed by 2) significance of improvement using 2nd-degree polynomial compared to 1st-degree polynomial transformations.

Threshold Identification

We utilized a modified Mazumdar^{2,3} method by expanding the search for optimal thresholds beyond a single point and by utilizing bootstrap resampling to validate distinct and significant thresholds. Thresholds were identified for each of TKV, htTKV, and BSA-TKV by iteratively evaluating all integers by increment of 1 unit across the 2.5th to 97.5th percentile of each TKV measurement. The first threshold was selected based on the significance of likelihood ratio test compared to a model without any threshold. The second threshold was assessed based on significance of likelihood ratio compared to a model with one threshold. This process was repeated 1,000 times using bootstrap resampling (R boot package v 1.3.28.1) to calculate bias, standard deviation, and frequency. We considered thresholds to be significant and distinct if they fall outside of the 95% confidence intervals of the other threshold (Figure S10).

Two Sample Mendelian Randomization

Independent genetic variants of outcomes and exposures at genome-wide significance ($P < 5 \times 10^{-8}$) were pruned based on linkage disequilibrium at a threshold of $r^2 < 0.001$ using the European subset of the 1000 Genomes phase 3 panel as the reference.⁴

Weighted-median, inverse-variance weighted, MR-Egger, heterogeneity, and intercept tests were performed using the R TwoSampleMR package (v 0.5.6). Directional pleiotropy was ascertained based on the significance ($P < 0.05$) of Egger intercept deviation from 0.⁵ MR-PRESSO was performed using the R MRPRESSO package (v 1.0). MR-PRESSO first assesses the presence of overall horizontal pleiotropy within a set of genetic instruments based on the significance of global test p-value ($P < 0.05$) and using 10,000 simulations.⁶ Subsequently, outlier and invalid variants with potential pleiotropic effects were identified and removed should the global test p-value reach significance. Instrument strength were estimated based on R^2 and F-statistic.

In forward MR, regression coefficients were converted from per 1 standard deviation (SD) increase in TKV to per 10 mL decrease in TKV by first multiplying -1, then dividing by 1 SD of TKV (unit in L) and multiplying by 10. In reverse MR, coefficients for eGFR and uACR were converted from per 1 logarithmic unit increase to per 10% reduction by multiplying -1 and the natural logarithm of 1.1. Coefficients for binary outcomes were converted from per 1 log odd increase to per 2-fold increase by multiplying the natural logarithm of 2.

Nonlinear Mendelian Randomization

Nonlinear Mendelian randomization (MR) analyses were performed using the R nlmr⁷ package (v 2.0). Residual TKV was calculated by subtracting genetically predicted TKV from observed TKV. Residual TKV was then stratified into deciles and localized average causal effects (LACE) were estimated while adjusting for age, sex, assessment centre, image processing protocol version, and the first 10 genetic PCs. Nonlinearity across LACE estimates were assessed using the fractional polynomial (FP), quadratic, and Cochran Q test.⁷ Validity of nonlinear MR result relies on the assumption of a constant instrumental variable and exposure relationship. Heterogeneity, or non-constant association between instrumental variable and exposure, were assessed using the Q test and quadratic trend test of heterogeneity (Table S11).

Figure S1: Histogram of TKV, htTKV, or BSA-TKV.

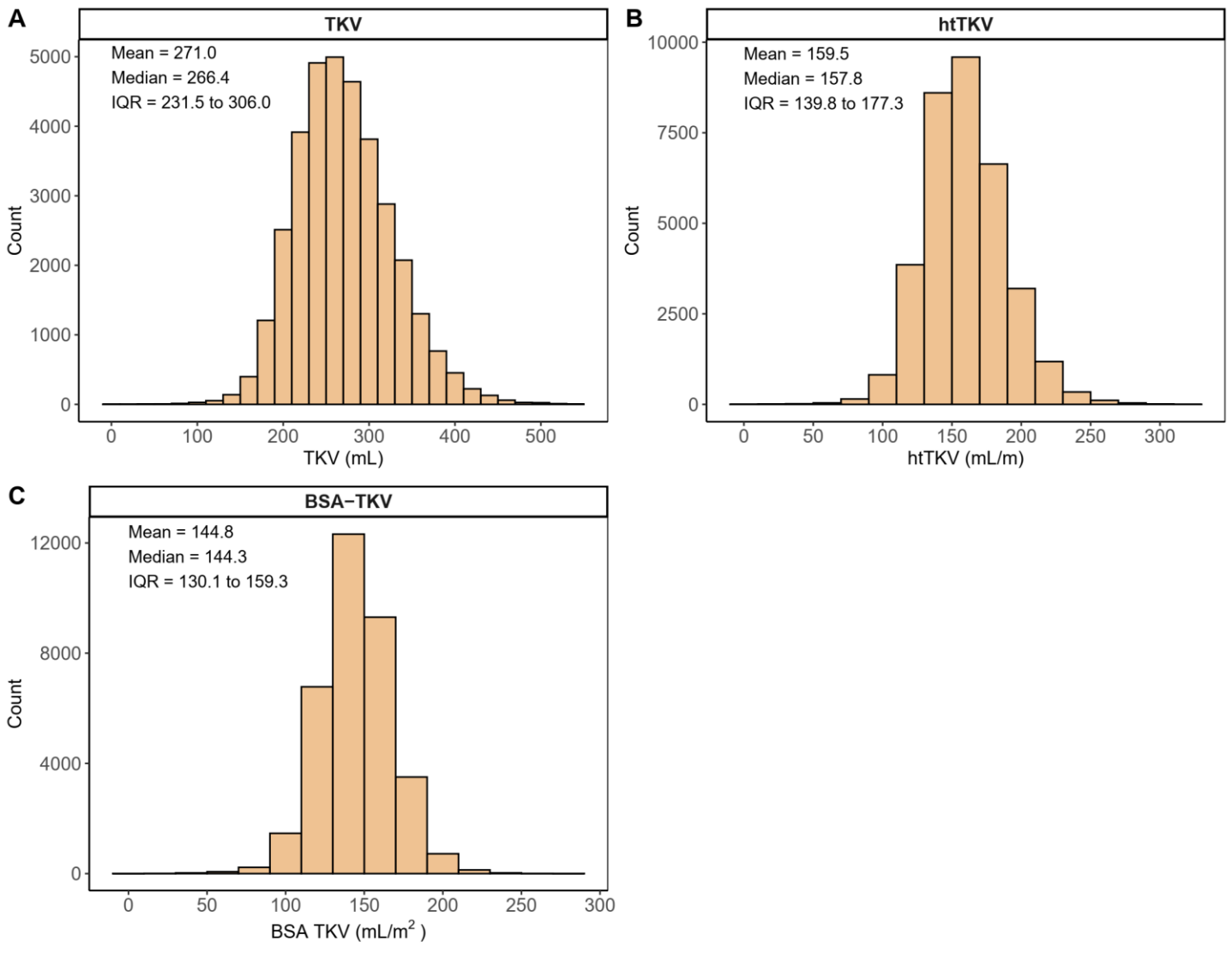
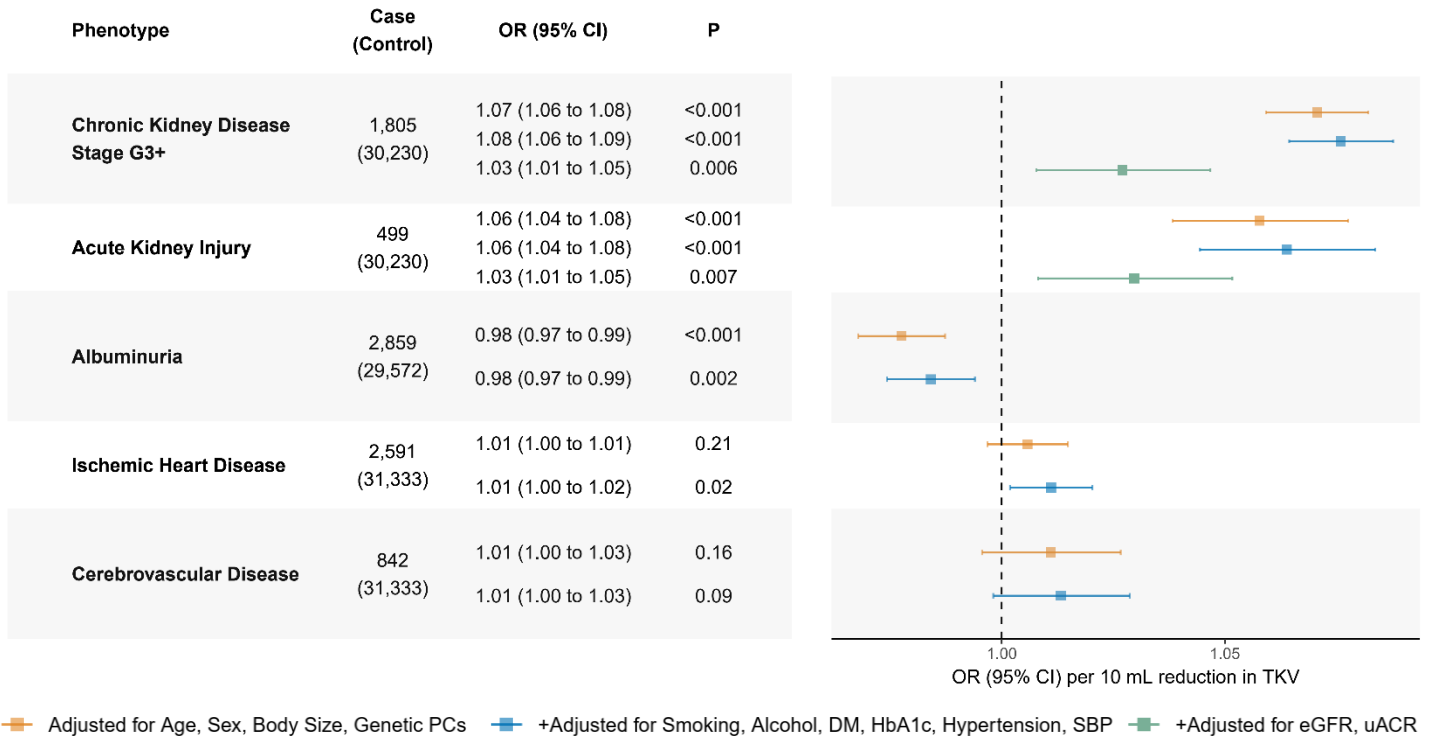
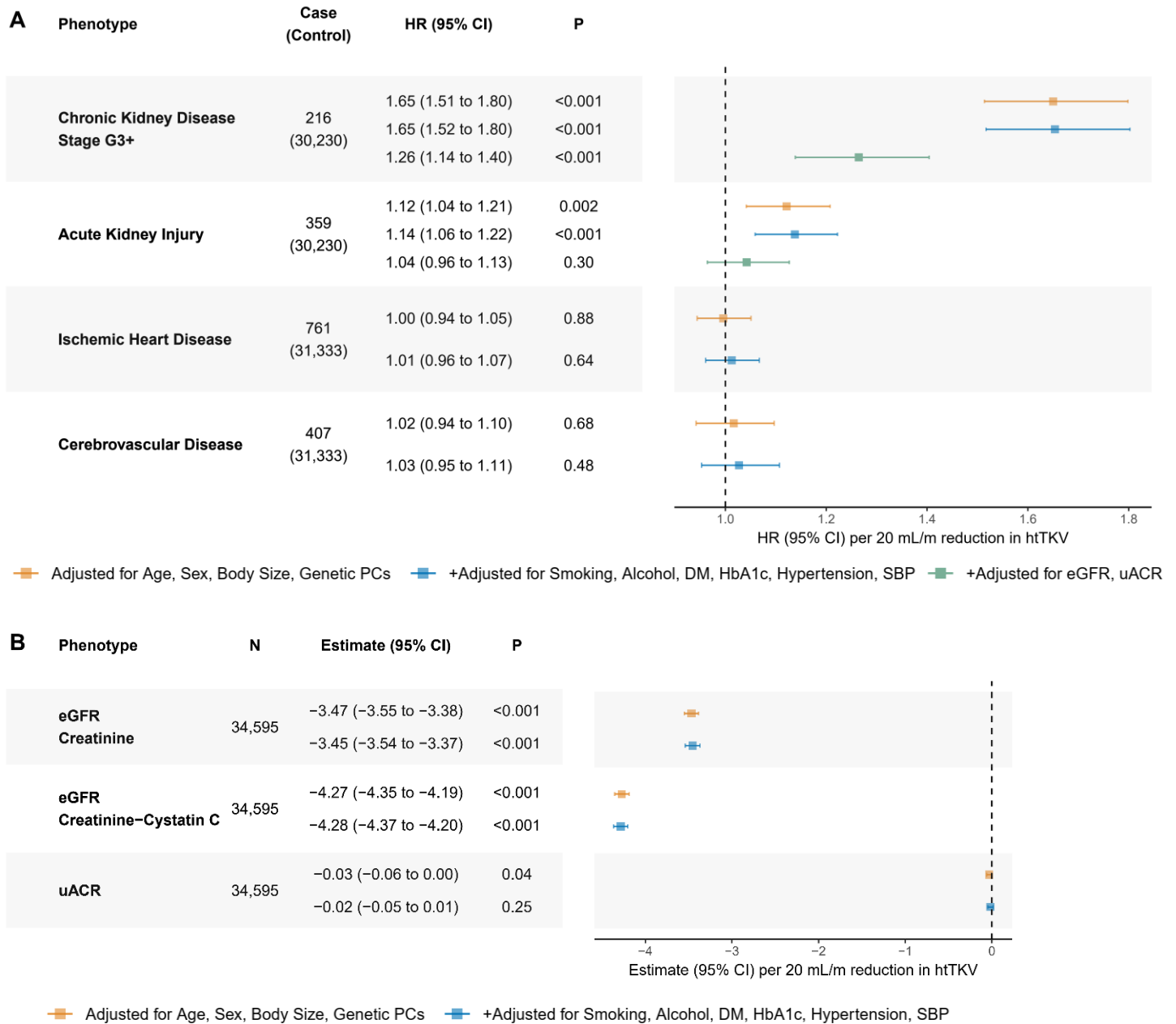


Figure S2: Association of TKV with all cases of kidney and cardiovascular disease outcomes.



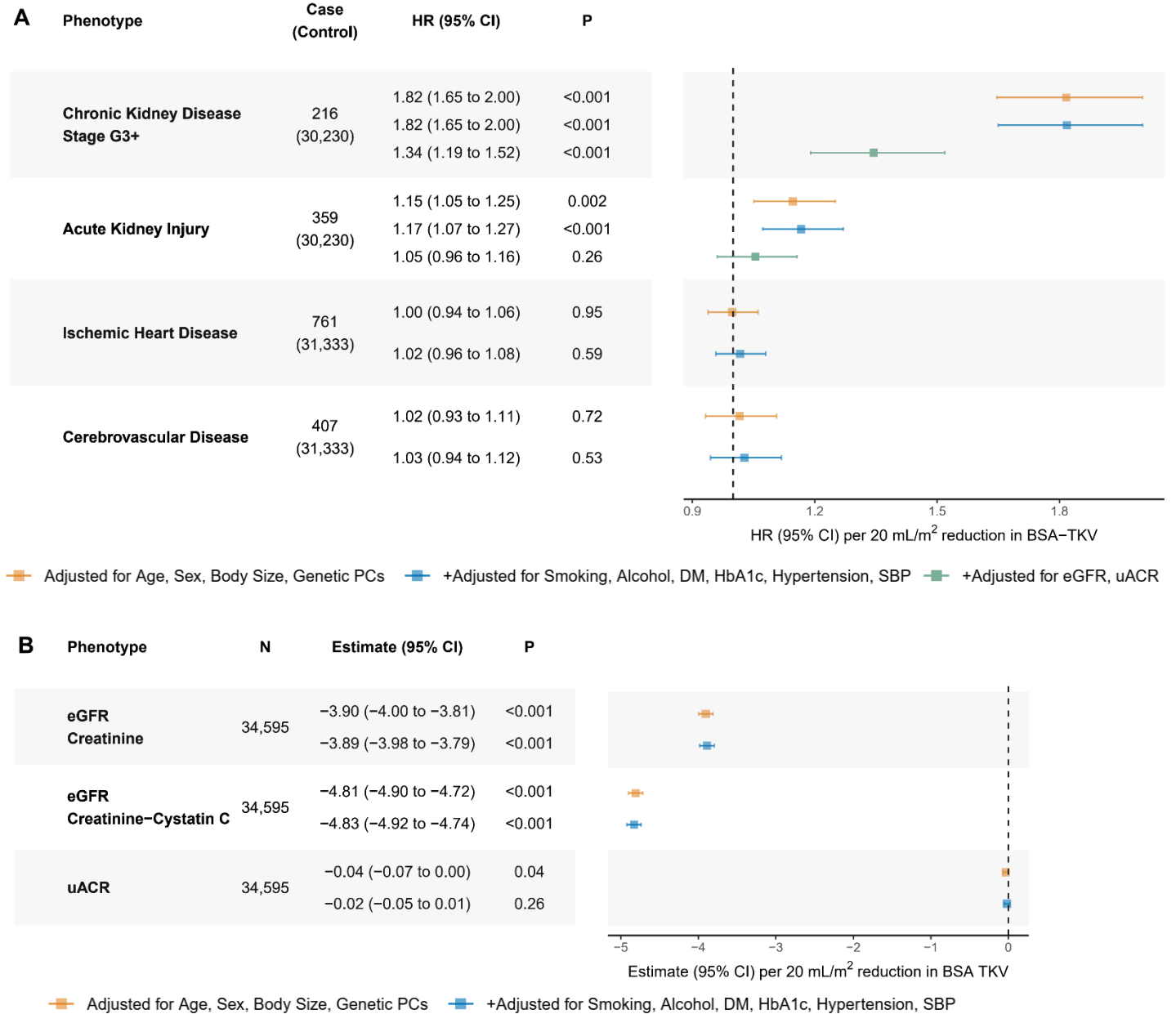
Association of TKV with all cases of disease outcomes were adjusted for 1) age, sex, body size including BMI and BSA, the first 10 genetic PCs of ancestry, image analysis protocol version and assessment centre, followed by 2) additionally adjusted for smoking, alcohol, DM, HbA1C, hypertension, and SBP. Association with CKD stage G3+ and AKI were further adjusted for eGFR and uACR. Significance threshold was corrected for multiple hypotheses testing based on the number of outcomes assessed.

Figure S3: Association of htTKV with kidney and cardiovascular disease outcomes and measures.



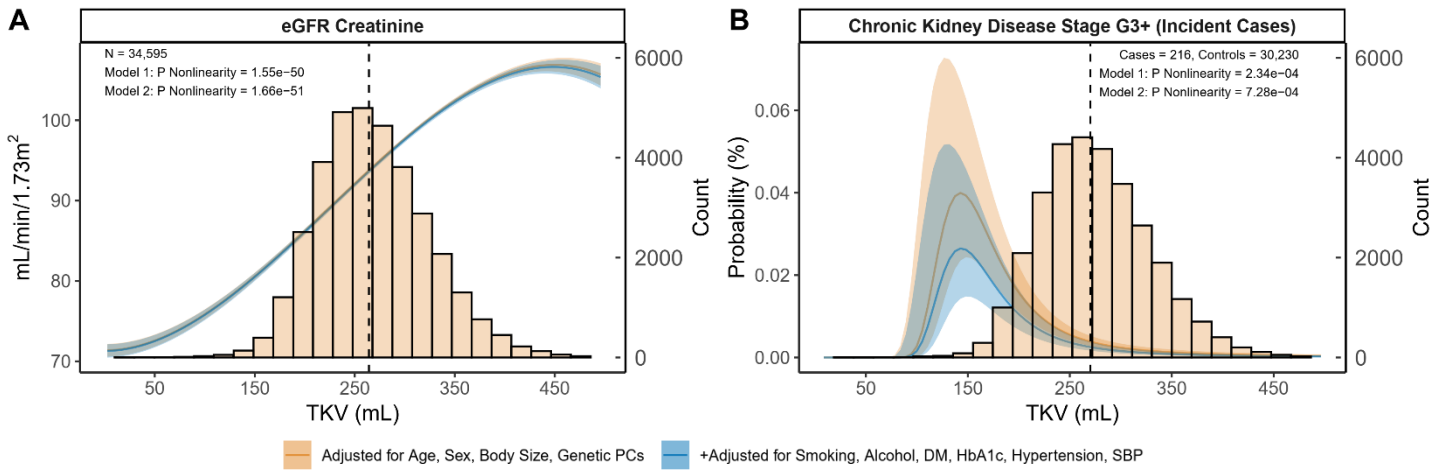
Association of htTKV with A) incident outcomes and B) kidney function biomarkers. Models were adjusted for 1) age, sex, body size including BMI and BSA, the first 10 genetic PCs, and nuisance factors including image analysis protocol version and assessment centre, followed by 2) additionally adjusted for smoking, alcohol, DM, HbA1C, hypertension, and SBP. Association with CKD stage G3+ and AKI were further adjusted for eGFR and uACR. Significance threshold was corrected for multiple hypotheses testing based on the number of outcomes assessed.

Figure S4: Association of BSA-TKV with kidney and cardiovascular disease outcomes and measures



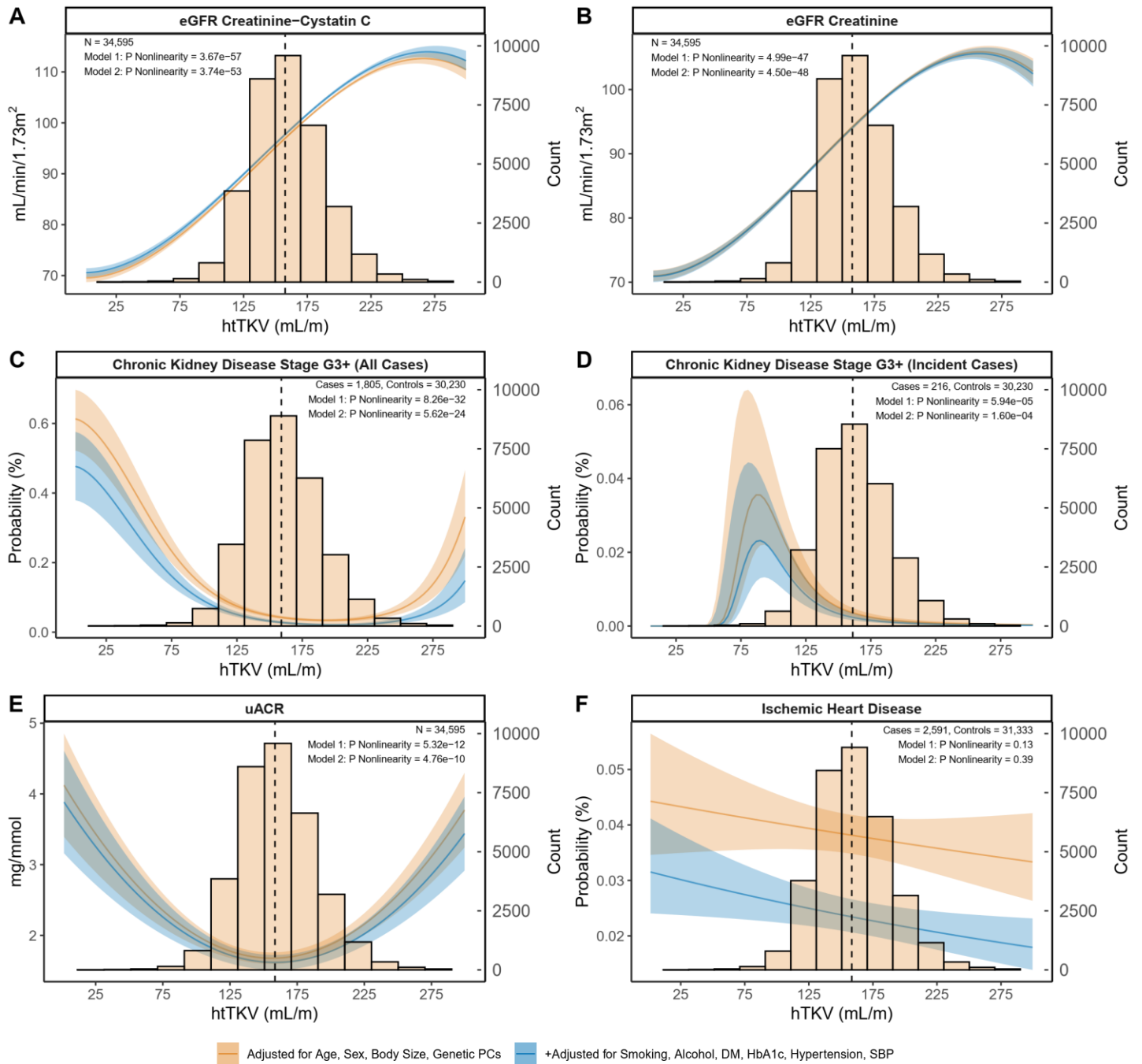
Association of BSA-TKV with A) incident outcomes and B) kidney function biomarkers. Models were adjusted for 1) age, sex, body size including BMI and BSA, the first 10 genetic PCs, and nuisance factors including image analysis protocol version and assessment centre, followed by 2) additionally adjusted for smoking, alcohol, DM, HbA1C, hypertension, and SBP. Association with CKD stage G3+ and AKI were further adjusted for eGFR and uACR. Significance threshold was corrected for multiple hypotheses testing based on the number of outcomes assessed.

Figure S5: Nonlinear association of TKV with eGFR_{Cr} and incident cases of CKD stage G3+.



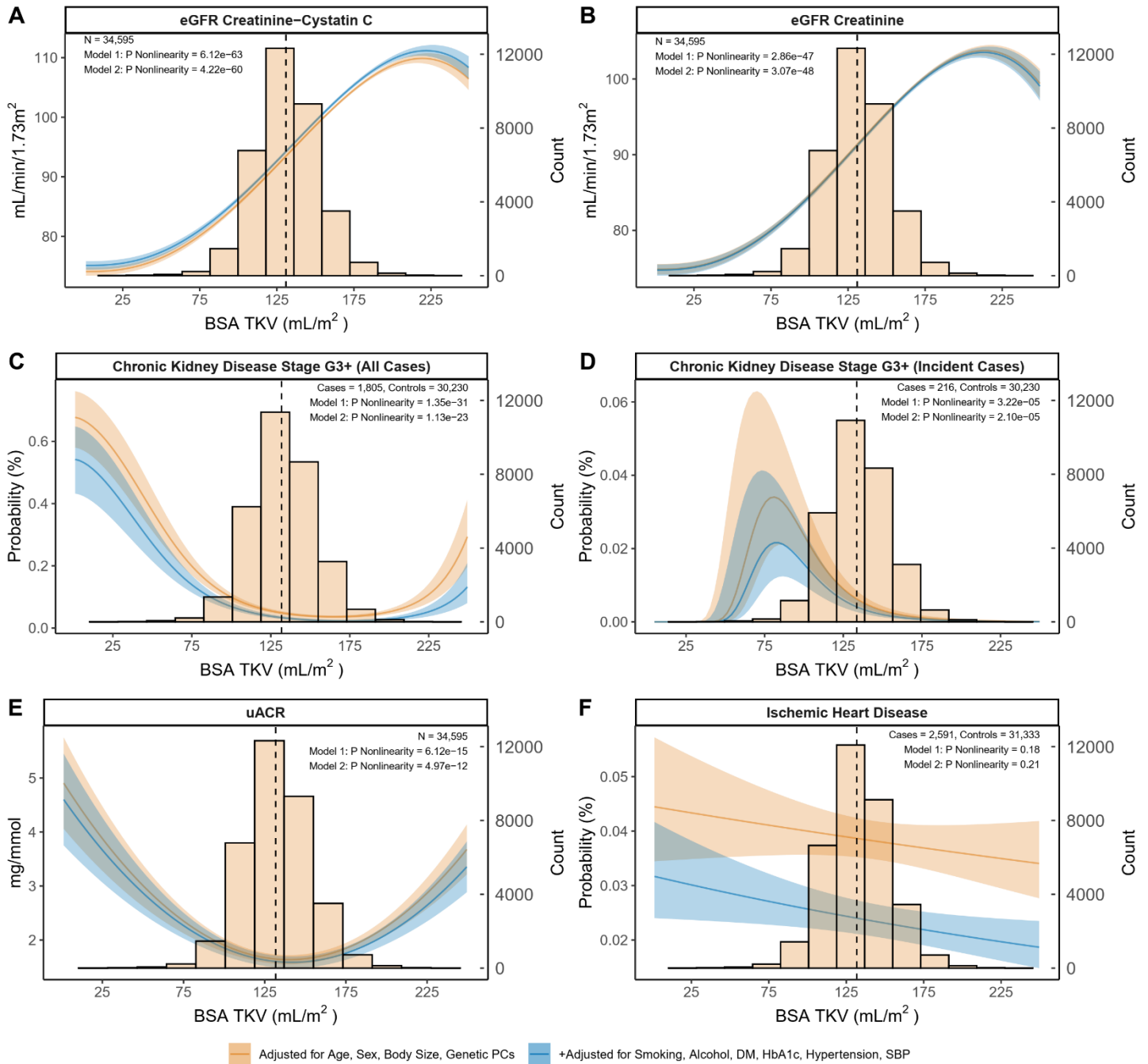
Model 1 was adjusted for age, sex, body size including BMI and BSA, and first 10 PCs. Model 2 was additionally adjusted for smoking, alcohol, DM, HbA1C, hypertension, and SBP. Dashed line marks the median of each histogram.

Figure S6: Nonlinear association of htTKV with kidney and cardiovascular disease outcomes and measures.



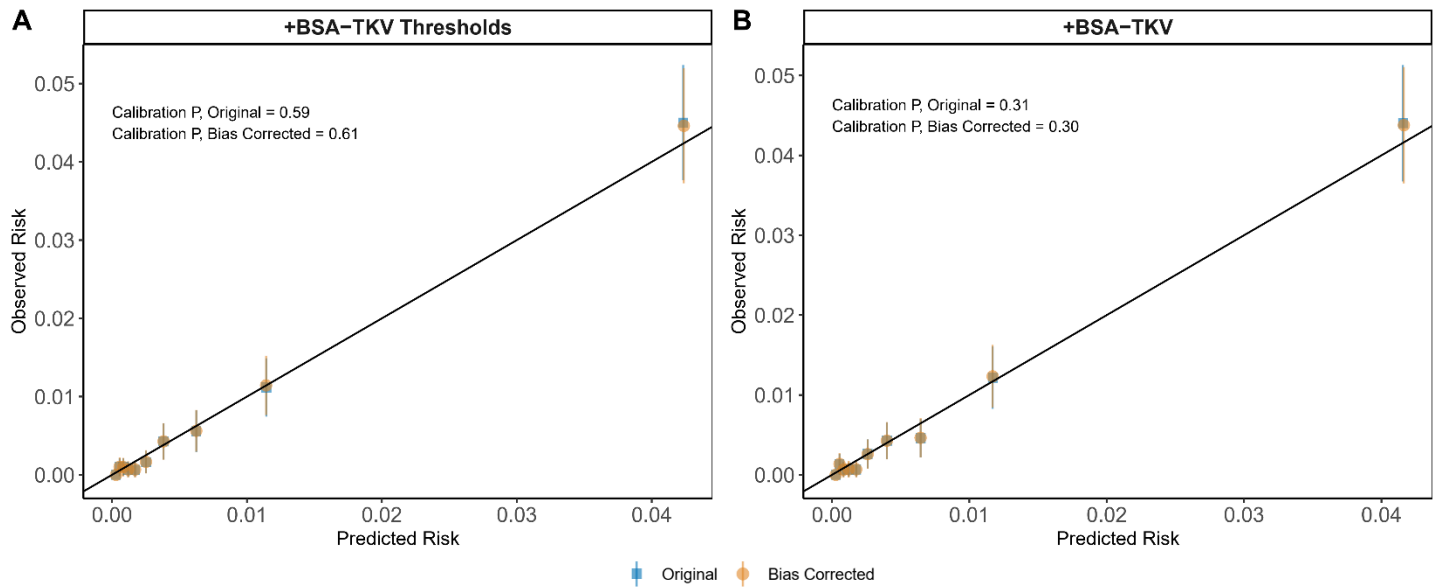
Model 1 was adjusted for age, sex, body size including BMI and BSA, and first 10 PCs. Model 2 was additionally adjusted for smoking, alcohol, DM, HbA1C, hypertension, and SBP. Dashed line marks the median of each histogram.

Figure S7: Nonlinear association of BSA-TKV with kidney and cardiovascular disease outcomes and measures.



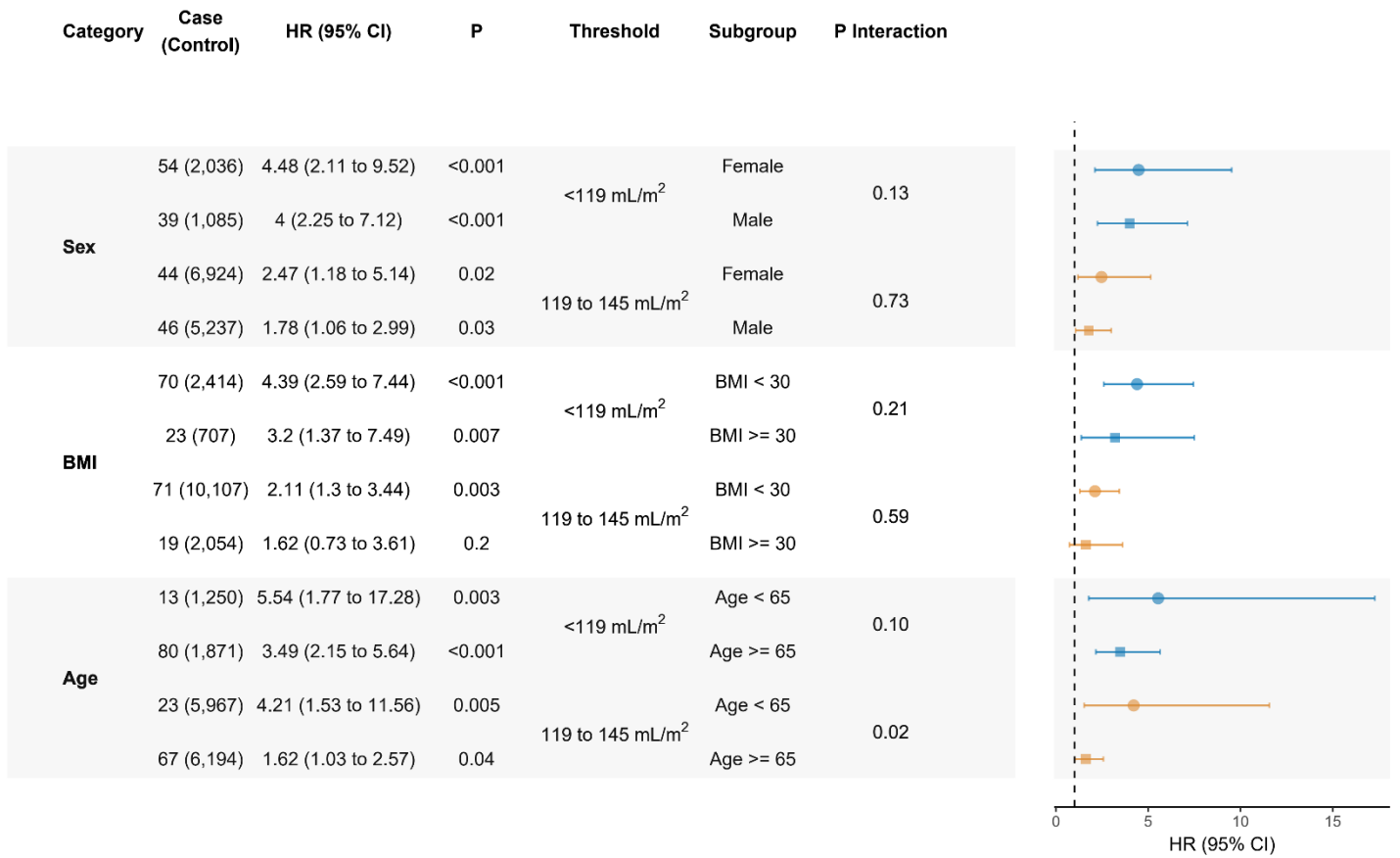
Model 1 was adjusted for age, sex, body size including BMI and BSA, and first 10 PCs. Model 2 was additionally adjusted for smoking, alcohol, DM, HbA1C, hypertension, and SBP. Dashed line marks the median of each histogram.

Figure S8: Calibration plot comparing observed and predicted risk when BSA-TKV is incorporated in a baseline model with eGFR and uACR.



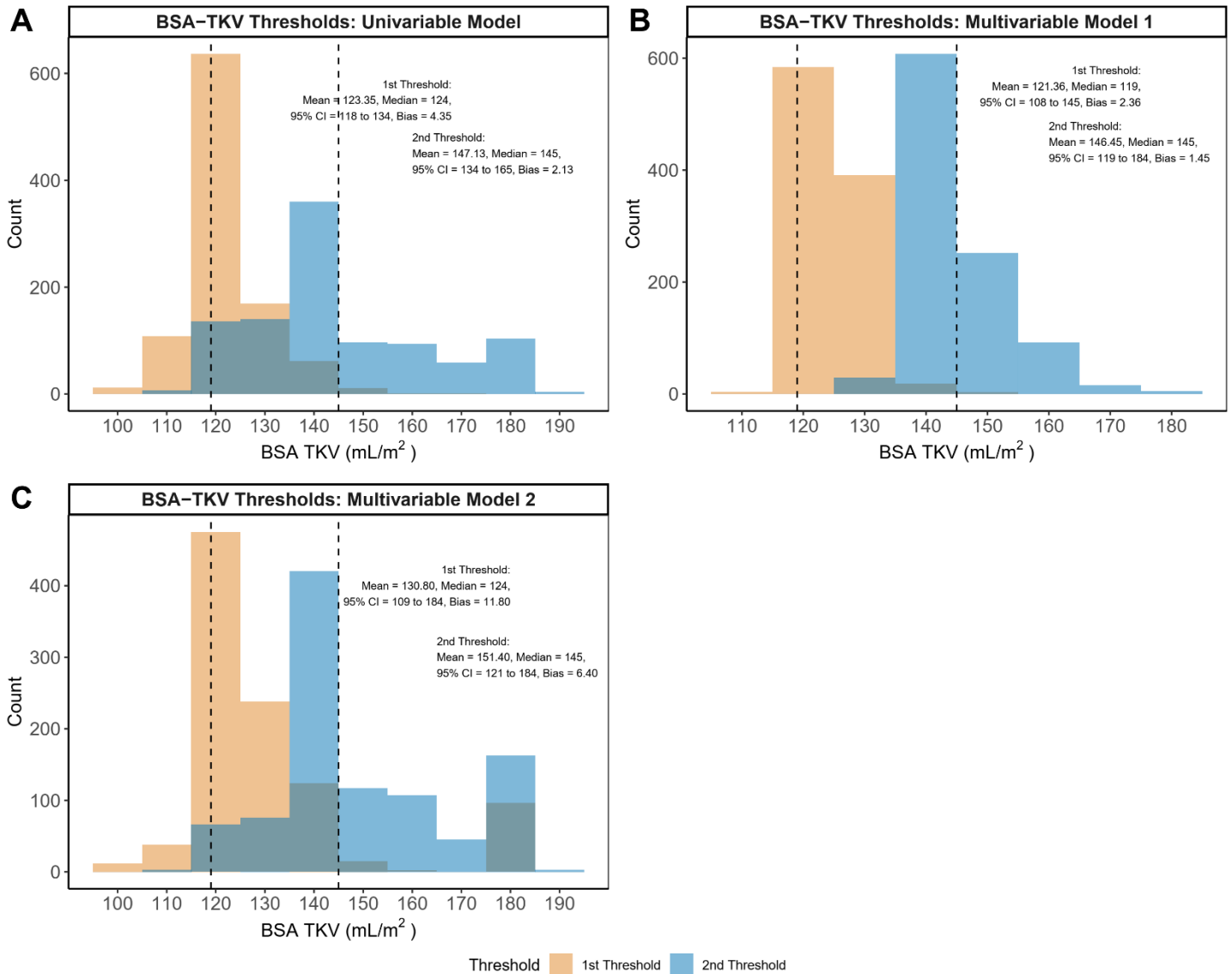
Significance of differences between predicted and observed risk was assessed using the Hosmer-Lemeshow test. Bias was corrected using Harrell's bias correction method.

Figure S9: Association of BSA-TKV thresholds with incident CKD stage G3+ split by age, sex, and BMI subgroups.



Analysis was adjusted for age, sex, body size including BMI and BSA, first 10 PCs, smoking, alcohol, DM, HbA1C, hypertension, SBP, eGFR and uACR. Significance threshold was adjusted for multiple hypotheses testing using Bonferroni correction based on the number of subgroups assessed.

Figure S10: Histogram and summary statistics of BSA-TKV thresholds identified from 1,000 iterations of bootstrap resampling.



Thresholds were identified in A) a univariable model consisting of only BSA-TKV thresholds, B) a multivariate model consisting of BSA-TKV thresholds in addition to eGFR and uACR, C) a multivariate model consisting of BSA-TKV thresholds, eGFR, uACR, age, sex, body size, smoking, alcohol, diabetes, HBA1c, hypertension, SBP, genetic PCs, analysis protocol, and stratified by assessment center. Dashed lines represent thresholds derived from the full cohort.

Table S1: Covariate sources and definitions.

Phenotype	FID	Category	Definition
Left Kidney Volume	21081	158	Left kidney volume
Right Kidney Volume	21082	158	Right kidney volume
Total Kidney Volume	NA	NA	Sum of left and right kidney volumes
Height Standardized Total Kidney Volume	NA	NA	Total kidney volume divided by height
Body Surface Area Standardized Total Kidney Volume	NA	NA	Total kidney volume divided by body surface area
IDP Pipeline Version	21094	158	Analysis protocol versions used to derive kidney volume
Assessment Centre	54	100113	Participant assessment center for UK Biobank recruitment
Age	21003	1001	Age of participants at time of assessment
Genetic Sex	22001	100313	Genetic sex determined by genotyping analysis
Genetic Principal Components	22009	716	Principal component scores derived from genotyping analysis
Smoking Status	20116	704	Self-reported current or past smoking status at time of assessment
Alcohol Intake Frequency	1558	704	Self-reported alcohol intake frequency at time of assessment
Systolic Blood Pressure	4080, 93	706	Two measures of blood pressure taken a few moments apart using either an automated machine or manual sphygmometer
Height	50, 12144	706	Standing height at time of assessment
Weight	3160, 21002, 23098	706	Body weight at time of assessment
BMI	21001	706	BMI at time of assessment
BSA	NA	NA	Body surface area based on the DuBois equation at time of assessment
HBA1c	30750	717	Hemoglobin A1c at time of initial, or if unavailable, follow-up assessment
Creatinine	30700	717	Creatinine at time of initial, or if unavailable, follow-up assessment
Cystatin C	30720	717	Cystatin C at time of initial, or if unavailable, follow-up assessment
eGFR Creatinine	NA	NA	eGFR creatinine calculated using CKD-EPI Creatinine Equation 2021
eGFR Creatinine and Cystatin C	NA	NA	eGFR creatinine calculated using CKD-EPI Creatinine-Cystatin Equation 2021
Urine Creatinine	30510	100083	Enzymatic creatinine in urine at time of initial, or if unavailable, follow-up assessment
Urine Microalbumin	30500	100083	Microalbumin in urine at time of initial, or if unavailable, follow-up assessment
uACR	NA	NA	Urine albumin-creatinine ratio calculated as ratio of urine microalbumin and urine creatinine

Table S2: Disease phenotype codes and definitions.

Disease Phenotype	Code (ICD10, OPCS4, UKB FID)	Definition
Chronic Kidney Disease Stage G3+	ICD10 N180, N183 - N185, Y602, Y841, Z490, Z491, Z492, Z992; OPCS4 X40 to X42; FID 42027	CKD stage 3 to stage 5, dialysis, algorithmically defined end-stage kidney disease, any eGFR < 60 mL/min/m ² , uACR > 30 mg/mmol
Acute Kidney Injury	ICD10 N170 - N179	Acute renal failure with tubular necrosis, acute renal failure with acute cortical necrosis, acute renal failure with medullary necrosis, other acute renal failure, acute renal failure (unspecified)
Ischemic Heart Disease	ICD10 I200, I21, I210, I211, I212, I213, I214, I219, I22, I220, I221, I228, I229, I23, I230, I231, I232, I233, I236, I238, I241, I252, I510, I513, I20, I201, I208, I209, I240, I251, Z951, Z955, I253, I254, I341, I25, I255, I256, I258, I259, I24, I248, I249	Angina pectoris, unstable angina, myocardial infarction, coronary atherosclerosis, other acute and subacute forms of ischemic heart disease, other chronic ischemic heart disease (unspecified), aneurysm and dissection of heart
Cerebrovascular Disease	ICD10 G454, G463, G464, G465, G466, G467, G468, I600, I677, I679, I68, I680, I682, I688, I65, I650, I651, I652, I653, I658, I659, I631, I632, I672, I63, I632, I635, I639, I66, I660, I661, I662, I663, I664, I668, I669, I676, I630, I633, I634, I635, I636, I638, I64, I67, I678, G450, G451, G452, G458, G459, G460, G461, G462, I675, I671, I69, I690, I691, I692, I693, I694, I698	Transient cerebral ischemia, cerebrovascular disease, occlusion of cerebral arteries, cerebral artery occlusion with cerebral infarction, occlusion and stenosis of precerebral arteries, cerebral ischemia, cerebral aneurysm, cerebral atherosclerosis, moyamoya disease, late effects of cerebrovascular disease
Diabetes Mellitus	ICD10 E10, E100, E106, E107, E108, E109, E101, E102, E103, E104, E11, E110, E116, E117, E118, E119, E13, E135, E136, E137, E138, E139, E149, E111, E131, E112, E103, E113, E123, E104, E114, E134, G590, Z964, R81, R824, G632, E103, E133, H360, R730, R739	Type 1 diabetes, type 1 diabetes with ketoacidosis, type 1 diabetes with renal manifestations, type 2 diabetes with ophthalmic manifestations, diabetic retinopathy, type 1 diabetes with neurological manifestations, type 2 diabetes with ketoacidosis, type 2 diabetes with renal manifestations, type 2 diabetes with ophthalmic manifestations, type 2 diabetes with neurological manifestations, type 2 diabetes, polyneuropathy in diabetes, impaired fasting glucose, other abnormal glucose, glycosuria or acetonuria, insulin pump user
Hypertension	ICD10 I10, I13, I130, I131, I132, I139, I11, I110, I119, I12, I120, I129, I15, I150, I151, I152, I158, I159, I674	Essential hypertension, hypertensive heart disease, hypertensive chronic kidney disease, hypertensive heart and/or renal disease, other hypertensive complications,

Table S3: Genetic variants associated with TKV above genome-wide significance.⁸

See supplemental Excel file.

Table S4: Summary of GWAS studies used in two-sample MR analyses.

See supplemental Excel file.

Table S5: Baseline demographic characteristics

Phenotype ^{a, b}	Quantity
TKV (mL)	266.44 (74.5)
hTKV (mL/m)	157.81 (37.55)
BSA TKV (mL/m ²)	144.5 (29.15)
Age (y)	64 (12)
Height (m)	1.69 (0.14)
Weight (kg)	74.9 (20.2)
BMI (kg/m ²)	25.91 (5.32)
BSA (m ²)	1.86 (0.3)
SBP (mmHg)	139 (26)
eGFR Creatinine-Cystatin C (mL/min/1.73m ²)	98.67 (17.62)
eGFR Creatinine (mL/min/1.73m ²)	98.03 (15.82)
uACR (mg/mmol)	1.07 (1.11)
HbA1C (%)	5.32 (0.44)
Sex	
Female	17835 (51.55)
Male	16760 (48.45)
CKD Stage G3+	1805 (5.22)
Acute Kidney Injury	499 (1.44)
Cerebrovascular Disease	842 (2.43)
Ischemic Heart Disease	2591 (7.49)
Type 2 Diabetes	1414 (4.09)
Hypertension	7131 (20.61)
Smoking	
Never	21590 (62.41)
Previous	11712 (33.85)
Current	1180 (3.41)
Alcohol	
Never	2084 (6.02)
<1 time/month	3359 (9.71)
1 to 3 times/month	3962 (11.45)
1 to 2 times/week	9250 (26.74)

3 to 4 times/week	9998 (28.9)
Daily or almost daily	5931 (17.14)

- a. Disease diagnoses include both incident and prevalent cases.
- b. Sex, disease diagnoses, smoking, and alcohol consumption frequency are expressed as number of individuals and percentage of cohort. All other variables are expressed as median and interquartile range.

Table S6: Discrimination, calibration, and likelihood ratio test assessing CKD Stage G3+ risk prediction performance of eGFR and uACR compared to model incorporating TKV measurements.

	C-Statistic	95% CI	DeLong P^a	Bias Corrected C-Statistic	Calibration P^a	Bias Corrected Calibration P^a	Likelihood Ratio Test P^a
eGFR + uACR	0.862	0.839 to 0.885	Reference	0.861	0.38	0.37	Reference
+TKV Thresholds	0.866	0.843 to 0.890	0.108	0.865	0.38	0.35	3.69E-05
+hTKV Thresholds	0.868	0.845 to 0.891	0.043	0.866	0.56	0.57	7.16E-06
+BSA TKV Thresholds	0.871	0.848 to 0.893	0.017	0.869	0.59	0.61	9.02E-08
+TKV	0.863	0.839 to 0.886	0.849	0.861	0.092	0.071	1.10E-02
+hTKV	0.863	0.840 to 0.887	0.588	0.862	0.084	0.087	3.24E-02
+BSA TKV	0.867	0.844 to 0.890	0.123	0.866	0.31	0.3	6.83E-06

a. Significance threshold corrected for multiple hypotheses testing = 0.05/3 or 0.017

Table S7: Improvement in category free risk reclassification when TKV, htTKV, or BSA-TKV were added to a baseline model of eGFR and uACR.

Category Free Net Reclassification Index	% ^a	95% CI	NARI ^b	P	Bias Corrected %	Bias Corrected NARI
TKV						
Event (n = 216)	15.74	2.57 to 28.91	1.12	0.019	15.67	1.11
Non-Event (n = 30,230)	1.02	-0.11 to 2.14	10.08	0.077	1.05	10.39
Total (n = 30,446)	16.76	3.54 to 29.97	11.2	0.013	16.72	11.5
htTKV						
Event (n = 216)	14.81	1.63 to 28.00	1.05	0.028	14.79	1.05
Non-Event (n = 30,230)	3.69	2.56 to 4.81	36.62	<0.001	3.73	37.06
Total (n = 30,446)	18.5	5.27 to 31.74	37.67	0.006	18.52	38.11
BSA-TKV						
Event (n = 216)	18.52	5.41 to 31.6	1.31	0.006	18.81	1.33
Non-Event (n = 30,230)	10.4	9.28 to 11.5	103.23	<0.001	10.44	103.62
Total (n = 30,446)	28.92	15.76 to 42.1	104.54	<0.001	29.24	104.95

- a. Percentage calculated as difference between number of individuals with increased risk score (if in the event cohort) and those with decreased risk score divided by number of individuals in event, non-event, or total category.
- b. Net absolute reclassification index was calculated as the product of reclassification percentage and event rate, multiplied by 1,000. Interpreted as absolute reclassification per 1,000 individuals.

Table S8: Inverse variance weighted, weighted median, and MR Egger regression results for each outcome associations using all SNPs.

See supplemental Excel file.

Table S9: Instrument strength, intercept test, and heterogeneity test results for each TKV-outcome association.

See supplemental Excel file.

Table S10: Inverse variance weighted, weighted median, and MR Egger results for each TKV-outcome association, excluding outlier SNPs identified by MR-PRESSO and BMI or BSA associated SNPs.

See supplemental Excel file.

Table S11: Nonlinear MR tests of nonlinearity and heterogeneity.⁷

See supplemental Excel file.

Table S12: Inverse variance weighted, weighted median, and MR Egger results for each genetically predicted exposure and TKV association.

See supplemental Excel file.

Table S13: Instrument strength, intercept test, and heterogeneity test results for each exposure-outcome association.

See supplemental Excel file.

Table S14: Inverse variance weighted, weighted median, and MR Egger results for each genetically predicted exposure and TKV association, excluding outlier variants identified by MR-PRESSO.

See supplemental Excel file.

Reference

1. Sauerbrei W, Meier-Hirmer C, Benner A, Royston P. Multivariable regression model building by using fractional polynomials: Description of SAS, STATA and R programs. *Comput Stat Data Anal*. 2006;50(12):3464-3485. doi:10.1016/j.csda.2005.07.015
2. Mazumdar M, Smith A, Bacik J. Methods for categorizing a prognostic variable in a multivariable setting. *Stat Med*. 2003;22(4):559-571. doi:10.1002/sim.1333
3. Duceppe E, Patel A, Chan MTV, et al. Preoperative N-Terminal Pro-B-Type Natriuretic Peptide and Cardiovascular Events After Noncardiac Surgery. *Ann Intern Med*. 2020;172(2):96-104. doi:10.7326/M19-2501
4. McVean GA, Altshuler (Co-Chair) DM, Durbin (Co-Chair) RM, et al. An integrated map of genetic variation from 1,092 human genomes. *Nature*. 2012;491(7422):56-65. doi:10.1038/nature11632
5. Burgess S, Thompson SG. Interpreting findings from Mendelian randomization using the MR-Egger method. *Eur J Epidemiol*. 2017;32(5):377-389. doi:10.1007/s10654-017-0255-x
6. Verbanck M, Chen CY, Neale B, Do R. Detection of widespread horizontal pleiotropy in causal relationships inferred from Mendelian randomization between complex traits and diseases. *Nat Genet*. 2018;50(5):693-698. doi:10.1038/s41588-018-0099-7
7. Staley JR, Burgess S. Semiparametric methods for estimation of a nonlinear exposure-outcome relationship using instrumental variables with application to Mendelian randomization. *Genet Epidemiol*. 2017;41(4):341-352. doi:10.1002/gepi.22041
8. Liu Y, Bastý N, Whitcher B, et al. Genetic architecture of 11 organ traits derived from abdominal MRI using deep learning. Janus ED, Barton M, Parisinos C, eds. *eLife*. 2021;10:e65554. doi:10.7554/eLife.65554